

CHAPTER 8 — USE OF DYNAMICAL CONCEPTS IN ASSESSING DEVELOPMENT

8.1 Basic ideas

- 8.1.1 Frontogenetic flow patterns
- 8.1.2 The two-layer model of the atmosphere

8.2 Ageostrophic motion

- 8.2.1 Definition
- 8.2.2 Vertical motion due to friction
- 8.2.3 Ageostrophic motion due to acceleration
 - 8.2.3.1 Acceleration/deceleration along the flow
 - 8.2.3.2 Curvature
 - 8.2.3.3 Isallobaric effects
 - 8.2.3.4 The latitude effect

8.3 Vorticity

- 8.3.1 Simplified vorticity equations
- 8.3.2 Vorticity advection
- 8.3.3 Local rate of change of vorticity

8.4 The development and movement of upper features

- 8.4.1 Thermal advection
- 8.4.2 Vorticity advection
- 8.4.3 Downstream development
- 8.4.4 Trough disruption
- 8.4.5 Blocking

8.5 Self development

- 8.5.1 Interaction of PVA with surface baroclinicity

8.6 The quasi-geostrophic omega equation

- 8.6.1 Discussion
 - 8.6.1.1 Interpretation: LHS
 - 8.6.1.2 Interpretation: RHS
- 8.6.2 Q vector form

8.7 Sutcliffe theory

- 8.7.1 Discussion
- 8.7.2 Interpretation

8.8 Potential vorticity (PV)

- 8.8.1 Potential vorticity; conservation, invertability
 - 8.8.1.1 Orographic and latitude effects
 - 8.8.1.2 Units and representation
- 8.8.2 The PV view of development

8.1 Basic ideas

8.1.1 Frontogenetic flow patterns

There are two main configurations of the synoptic-scale horizontal flow in relation to a pre-existing thermal gradient which act to increase the baroclinicity. These deformation patterns fall into two categories:

- (i) Diffluence in the flow across a thermal gradient. (Fig. 8.1(a), Fig. 8.1(c)).
- (ii) Shear in the flow leading to the tilting of the orientation of a thermal gradient. (Fig. 8.1(b), Fig. 8.1(c). See also Fig. 8.11.)

Since the thermal wind is the major component of the upper tropospheric wind in baroclinic zones, these frontogenetic effects strengthen upper-level winds.

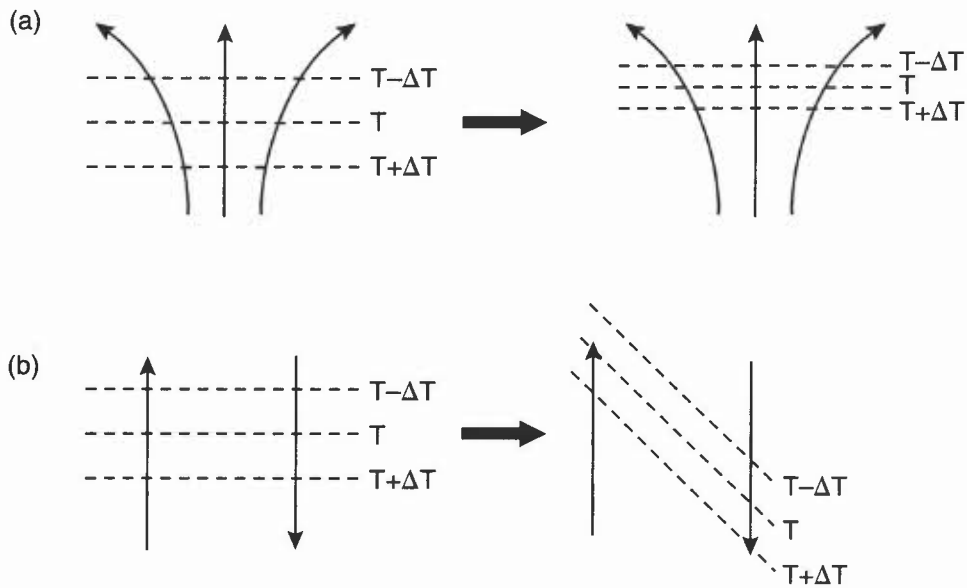


Figure 8.1. Deformation patterns associated with frontogenesis. (a) Diffluence, and (b) shear.

8.1.2 The two-layer model of the atmosphere

In situations of active development, the atmosphere may be divided into two layers of opposite divergence, separated by a level of non-divergence (Fig. 8.2). This simple schematic model is valid for regions with strong vertical velocity through the troposphere and marked changes in surface pressure; it has the following characteristics:

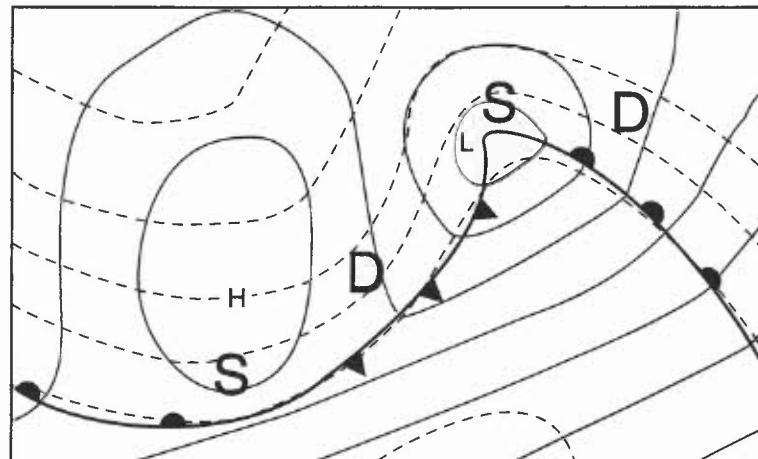


Figure 8.2. Mean sea-level pressure (solid lines) and thickness (dashed lines). Regions of diffluence and shear frontogenesis marked by D and S, respectively.

- (i) The upper-level divergence is stronger than that at lower levels, and drives the circulation.
- (ii) Vertical motion is at a maximum at the level of non-divergence, falling to zero at the surface and at some upper level, nominally the tropopause.

Subjective methods of assessing surface development are based on this model, and often rely on the diagnosis of upper-level divergence via either ageostrophic motion or vorticity.

8.2 Ageostrophic motion

8.2.1 Definition and significance

The ageostrophic wind is that part of the wind not in geostrophic balance, i.e. the wind associated with an imbalance between Coriolis force (acting to the right of the motion in the northern hemisphere and proportional to the wind speed) and pressure gradient force (acting down the pressure gradient). Its chief practical significance lies in the fact that by identifying it, we isolate the component of the horizontal wind field causing vertical motion.

8.2.2 Vertical motion due to friction

- (i) Friction deflects the wind towards lower pressure and reduces its strength. In cyclonic (anticyclonic) flow within the boundary layer, ageostrophic motion due to friction causes convergence (divergence).
- (ii) Unlike situations of large-scale ascent, the resulting vertical velocity is generally only of order of millimetres per second and is at a maximum at the top of the boundary layer, where it is proportional to the geostrophic relative vorticity.
- (iii) An opposite but weaker divergence profile compensates above the boundary layer (**Fig. 8.3**).

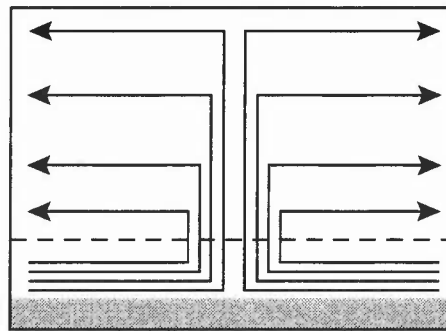


Figure 8.3. Streamlines of frictionally induced motion in cyclonic flow. (The dashed line indicates the top of the boundary layer.)

8.2.3 Ageostrophic motion due to acceleration

- (i) Imbalance between Coriolis force and pressure gradient force gives ageostrophic motion with magnitude proportional to the acceleration of the flow, acting to the left of the acceleration vector in the northern hemisphere.
- (ii) The total time derivative of the wind velocity, i.e. the acceleration, can be split into local and advective components, giving local, or *isallobaric* and advective, or *downwind* changes in velocity, respectively. The downwind effects can be further subdivided into along-flow acceleration and curvature effects.

8.2.3.1 Acceleration/deceleration along the flow

- (i) This component of ageostrophic motion is directed across the flow, and its strength can be gauged on a chart showing gph contours and isotachs — the smaller the areas bounded by contours and isotachs, the larger the ageostrophic motion.
- (ii) It results in upper-level divergence and surface cyclonic development areas at right entrances and left exits of jets, with upper-level convergence and surface anticyclonic development areas at left entrances and right exits (**Fig. 8.4**).

8.2.3.2 Curvature

- (i) This component of ageostrophic motion is directed against the flow in cyclonic curvature and with the flow in anticyclonic curvature. Adding it to the geostrophic wind gives the gradient wind.
- (ii) Consideration of this effect gives upper-level divergence (convergence) and surface cyclonic (anticyclonic) developments areas where curvature is becoming more anticyclonic (cyclonic) or less cyclonic (anticyclonic) along the flow (**Fig. 8.5**).

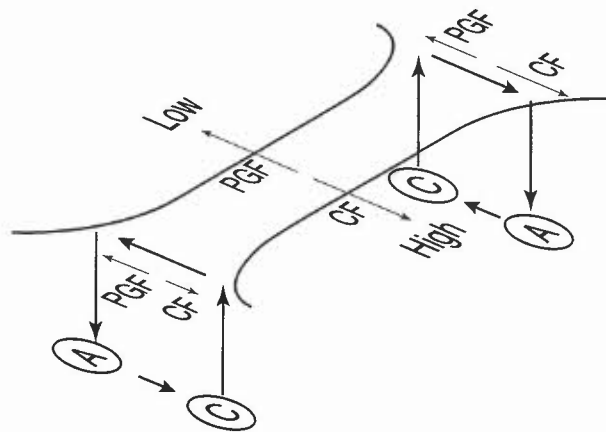


Figure 8.4. Ageostrophic motion, vertical velocity and development areas associated with a jet. Ageostrophic motion at upper levels associated with downwind acceleration, at lower levels with isallobaric effects. Also shown are changes in relative strengths of pressure gradient and Coriolis forces.

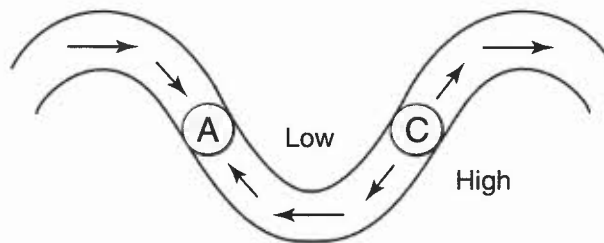


Figure 8.5. Ageostrophic motion and development areas associated with an upper trough-ridge flow pattern.

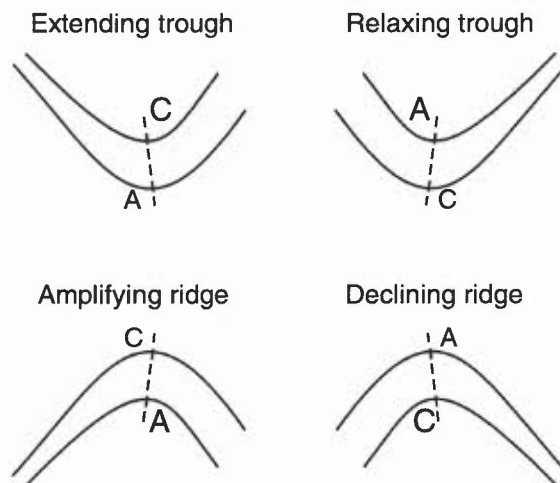


Figure 8.6. Major and minor development areas due to downwind changes. Also indicated are tendencies induced in upper-level flow patterns.

Combining the two types of downwind changes leads to major and minor cyclonic (C) and anticyclonic (A) development areas in association with the different combinations of confluence and diffluence with cyclonic and anticyclonic curvature (**Fig. 8.6**).

8.2.3.3 Isallobaric effects

- (i) These arise from local changes in the pressure gradient force; the resulting ageostrophic motion is directed down the isallobaric gradient. At the surface isallobaric flow is directed into regions of pressure falls and away from regions of pressure rises (**Fig. 8.4**).
- (ii) At upper levels, the most significant cause of isallobaric motion is horizontal variation in thermal advection.

- (iii) Warm advection tends to raise upper-level geopotential height. This results in isallobaric motion directed away from the warm advection maximum, with attendant divergence aloft and ascent through the atmospheric column (**Fig. 8.7(a)**).
- (iv) Cold advection has the opposite affect, with upper-level convergence and descent (**Fig. 8.7(b)**).
- (v) On the edges of advection areas, the opposite sign of divergence tends to occur. For instance, cold advection behind a cold front contributes to ascent at the front (**Fig. 8.8**).
- (vi) During the process of frontogenesis, parcels of air are being accelerated, as at a jet entrance, leading to isallobaric motion from warm to cold air (**Fig. 8.7(c)**). For this reason cloud and rain are often confined to the warm side of the jet, with clear air on the cold side.

The static stability of the air modulates these motions; if the air is stable, ascent (descent) produces marked cooling (warming) which offsets the advective changes in potential temperature. In addition, sources of heat can be important in producing divergence.

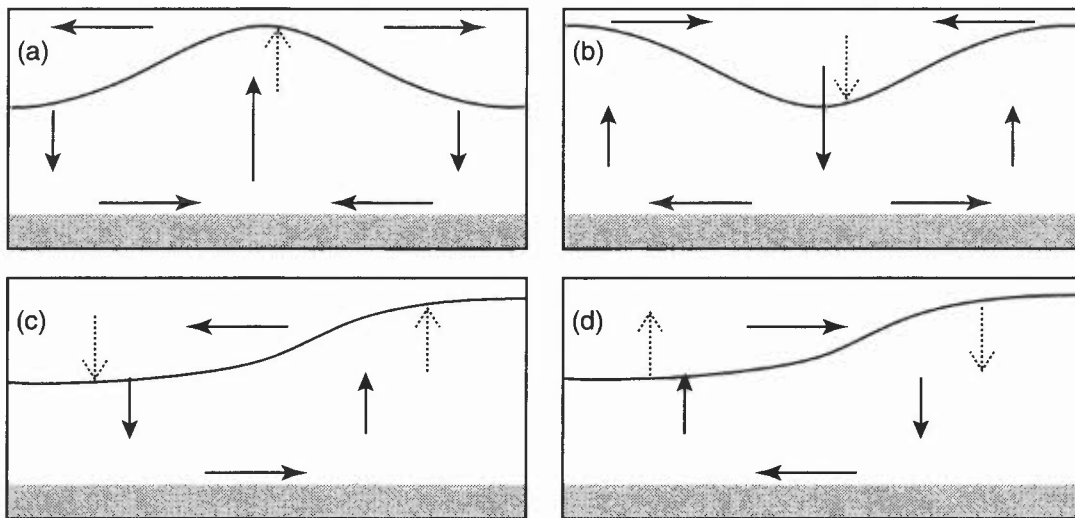


Figure 8.7. Cross-sectional views of upper-tropospheric pressure surfaces and direction of instantaneous change in height (dotted arrows). Resulting departure from geostrophic balance and induced vertical motion is shown by solid arrows. (a) Warm advection, (b) cold advection, (c) jet entrance (following motion) or frontogenesis, and (d) jet exit (following motion) or frontolysis.

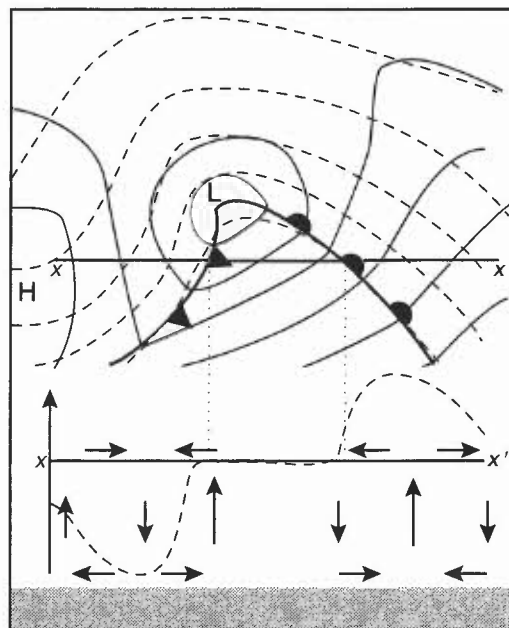


Figure 8.8. Top: contours of mean sea-level pressure (solid) and thickness (dashed) associated with a schematic developing warm-sector depression. Bottom: upper-level gph tendency due to thermal advection along line XX' (dashed) and cross-section of resulting ageostrophic and vertical acceleration (arrows).

8.2.3.4 The latitude effect

- (i) Since the geostrophic wind is inversely proportional to f , and thus to the sine of the latitude, for a given pressure gradient, the geostrophic wind will increase in strength as the equator is approached and decrease in strength as the pole is approached.
- (ii) Thus cyclonic (anticyclonic) development is favoured by a strong equatorward (poleward) flow, and there is a tendency for retrogression of large-amplitude, long-wave troughs and ridges against the usual west–east current (Fig. 8.9).

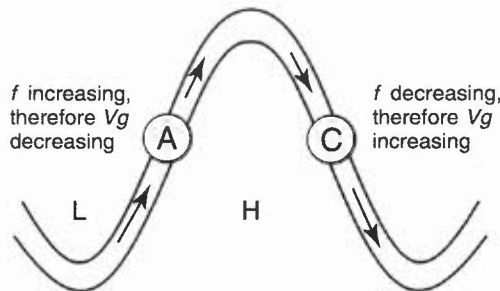


Figure 8.9. Development areas due to the divergence/convergence of the geostrophic wind with large changes in latitude, leading to tendency for retrogression.

8.3 Vorticity

8.3.1 Simplified vorticity equations

- (i) A simplified vorticity equation (SVE) offers an alternative way of diagnosing divergence without reference to ageostrophic motion. It shows the fractional rate of change of absolute vorticity following the motion to be proportional to the convergence (ignoring frictional effects and the tilting of horizontal vorticity).

$$\frac{1}{\zeta + f} \frac{d(\zeta + f)}{dt} \approx -\text{div}_H \mathbf{V}$$

- (ii) This equation is most easily visualized as the ‘ice-skater’ effect, whereby ice skaters increase their vorticity (= angular velocity) through drawing their arms in (convergence) and decrease it through stretching their arms out (divergence), e.g. convergence in the lower part of the frontogenetic circulation illustrated in Fig. 8.7(c) generates vorticity, manifested as a pressure trough marking the surface front.
- (iii) Splitting the total rate of change of absolute vorticity into local and advective components shows that divergence is associated with the advection of vorticity and the local rate of change of vorticity.

$$-\text{div}_H \mathbf{V} \approx \underbrace{\frac{1}{\zeta + f}}_{\text{convergence}} \left(\underbrace{\frac{\partial \zeta}{\partial t}}_{\text{local rate of change of vorticity}} + \underbrace{\mathbf{V} \cdot \nabla(\zeta + f)}_{\text{vorticity advection}} \right)$$

8.3.2 Vorticity advection

- (i) Positive (negative) vorticity advection contributes towards divergence (convergence).
- (ii) Vorticity advection gives the same regions of divergence diagnosed by consideration of ageostrophic motion due to downwind acceleration. Advection of shear vorticity gives divergence due to ageostrophic motion resulting from along-flow acceleration/deceleration, whilst advection of curvature vorticity gives divergence due to ageostrophic motion resulting from curvature.
- (iii) The advection of planetary vorticity (f) is also entirely equivalent to the latitude effect discussed in 8.2.3.4, e.g. a northerly flow gives positive vorticity advection and a cyclonic development area.

8.3.3 Local rate of change of vorticity

- (i) Horizontal variations in thermal advection beneath an upper pressure level cause vorticity to change at a point. Over a maximum of warm (cold) advection absolute vorticity decreases (increases); the SVE shows this change to be accompanied by divergence (convergence).
- (ii) Such changes have their direct equivalent in the isallobaric effects discussed in 8.2.3.3. As shown in that section, divergence of the opposite sign tends to occur on the periphery of the region of thermal advection.
- (iii) It is best to consider thickness advection through a deep layer, preferably the whole of the troposphere. This can be assessed using a representation of 300 or 250 hPa gph contours superimposed on mean sea-level pressure. Low-level flow from low (high) to high (low) upper-level gph indicates cold (warm) advection, whilst the smaller the areas formed between two gph contours and two isobars, the stronger the advection.
- (iv) On average, vorticity advection is more influential than thermal advection in producing mid-tropospheric vertical velocity. Thermal advection is at its most effective somewhat lower down, say at 700 hPa .

8.4 The development and movement of upper features

8.4.1 Thermal advection

- (i) Thermal advection tends to induce opposite gph tendencies at lower and upper levels, e.g. warm advection is often associated with falling surface pressure but rising 300 hPa gph because of the increasing thickness. At some mid-level, the level of non-divergence (on average 500–600 hPa), it has a smaller, indeterminate effect.
- (ii) Adiabatic and diabatic heating/cooling can act to offset advective changes, e.g. cold advection to the west of the UK in winter can be significantly offset by diabatic warming through convection and adiabatic warming through descent, limiting the amount of cooling in the column and thus the fall of upper-level gph.

8.4.2 Vorticity advection

- (i) Positive (negative) vorticity advection favours falling (rising) surface pressure and thus, ignoring the effects of any changes in temperature in the atmospheric column, falling (rising) upper-level gph.
- (ii) For example, a diffluent upper trough leads to falling surface gph downstream of its axis on its cold side, and this is reflected by a fall in gph at upper levels. Such troughs, therefore, tend to extend and sharpen. One way to look at this process is as the advection of shear vorticity and planetary vorticity into the axis of the trough, reinforcing it. **Fig. 8.6** shows this and other configurations.
- (iii) The divergence field due to advection of curvature vorticity leads to progression of troughs and ridges, shorter-wavelength features moving most quickly. Similarly, the divergence field due to shear vorticity advection causes a jet to progress through the pattern.
- (iv) Planetary-scale troughs and ridges tend to be slow moving or stationary under a balance between curvature and planetary vorticity advection, whereas the shorter-wavelength features associated with travelling weather systems move through the pattern. (Because of the cancellation between relative vorticity advection and planetary vorticity advection associated with the planetary-scale features, the usual configuration of ‘A’ and ‘C’ areas does not apply.)
- (v) At the nominal level of non-divergence, vorticity is conserved following the motion. For this reason vorticity features are advected around and often preserve their identities longer on a 500 hPa chart than on a 250 hPa chart.

The following table summarizes and compares the factors leading to changes in geopotential height near the surface and in the upper troposphere.

Development	Factors favouring
Surface C area	PVA + centre of warm advection area or where cold advection area borders on region of little thermal advection.
Surface A area	NVA + centre of cold advection area or where warm advection area borders on region of little thermal advection.
Upper-level C area	PVA + cold advection.
Upper-level A area	NVA + warm advection.

NB. PVA and NVA refer to the upper-tropospheric vorticity advection.

In any instance, thermal advection may be acting to offset vorticity advection.

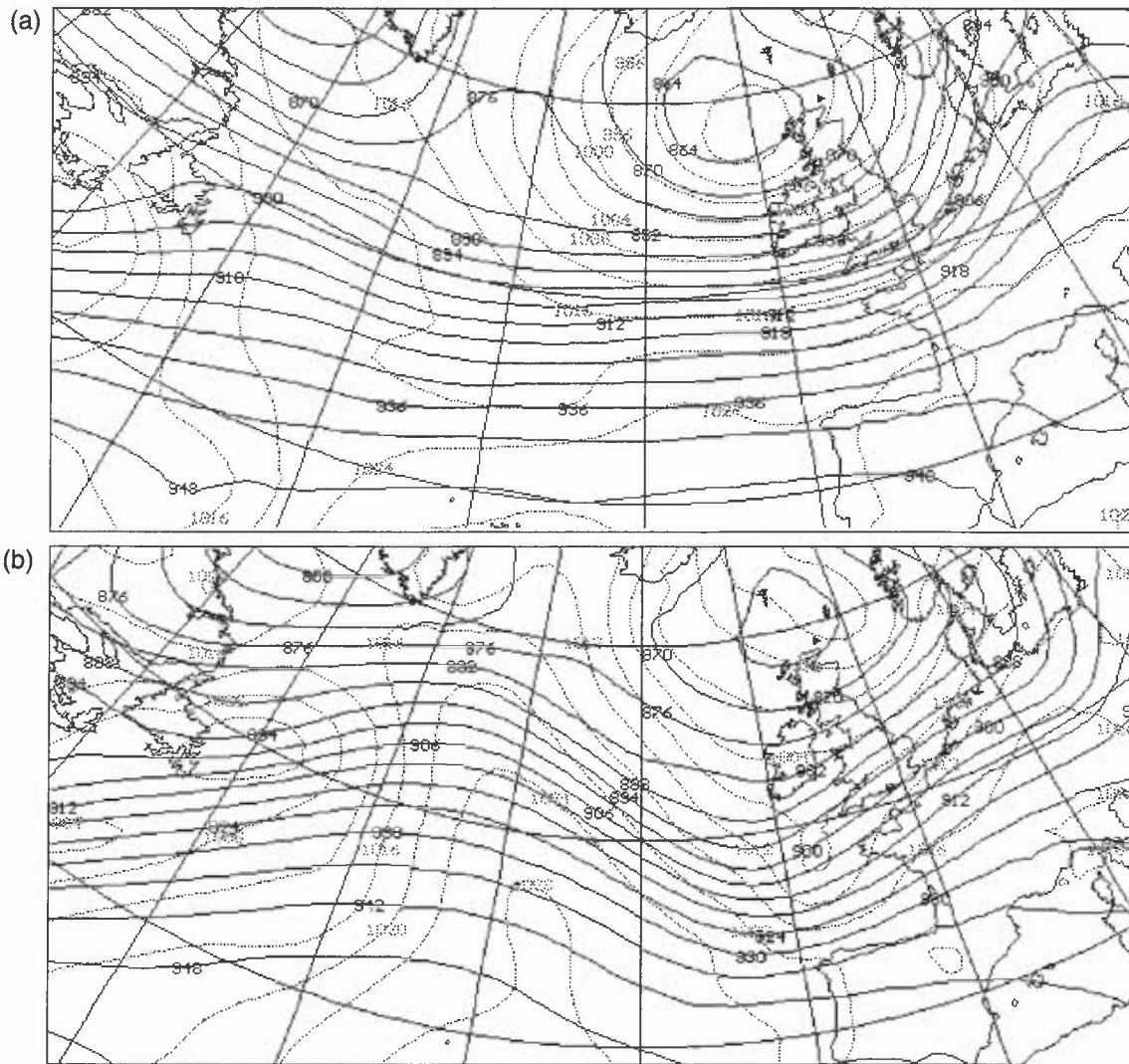


Figure 8.10. Development in the north-east Atlantic downstream of strong, warm advection in the north-west Atlantic. Dark lines; 300 hPa gph every 6 dam, lighter lines: MSLP every 4 hPa. Above 0000 UTC on 27 April 1992, below 2100 UTC on 27 April 1992. Thermal advection strength can be gauged by the smallness of the areas bounded by two MSLP and two 300 gph contours, a surface flow from high to low 300 hPa gph indicating warm advection.

8.4.3 Downstream development

Weather systems can be influenced by events upstream on a time scale shorter than that in which advective processes can account for their development. A typical process is now described:

- (i) A vigorous surface depression generates much warm advection ahead of it, which builds an upper ridge.
- (ii) The consequent veering of the thermal gradient downstream of the ridge axis leads to a tightening of that gradient through shear frontogenesis, so the jet strengthens.
- (iii) The resulting downstream diffluent trough extends and sharpens through advection of cyclonic shear vorticity into its axis, and gives rise to a new cyclonic surface development.
- (iv) The intensification of this new surface feature induces cold advection on its western flank, reinforcing the upper trough.
- (v) This sequence is contributory in determining the evolution shown in **Fig. 8.10**.

8.4.4 Trough disruption

- (i) Trough disruption is said to occur when the poleward portion of a trough becomes separated from the equatorward part and moves on, often having left a cut-off circulation (**Fig. 8.11**).
- (ii) This evolution sometimes follows the extension of a trough, especially if sufficient positive vorticity, both planetary and shear, is advected into the lower part of the trough, or if a cut-off region of cold air due to strong cold advection forms in the region of the trough.
- (iii) The induced cyclonic circulation brings warmer air of originally lower planetary vorticity around its eastern then northern flanks, and it thus cuts itself off from the higher-vorticity polar air.

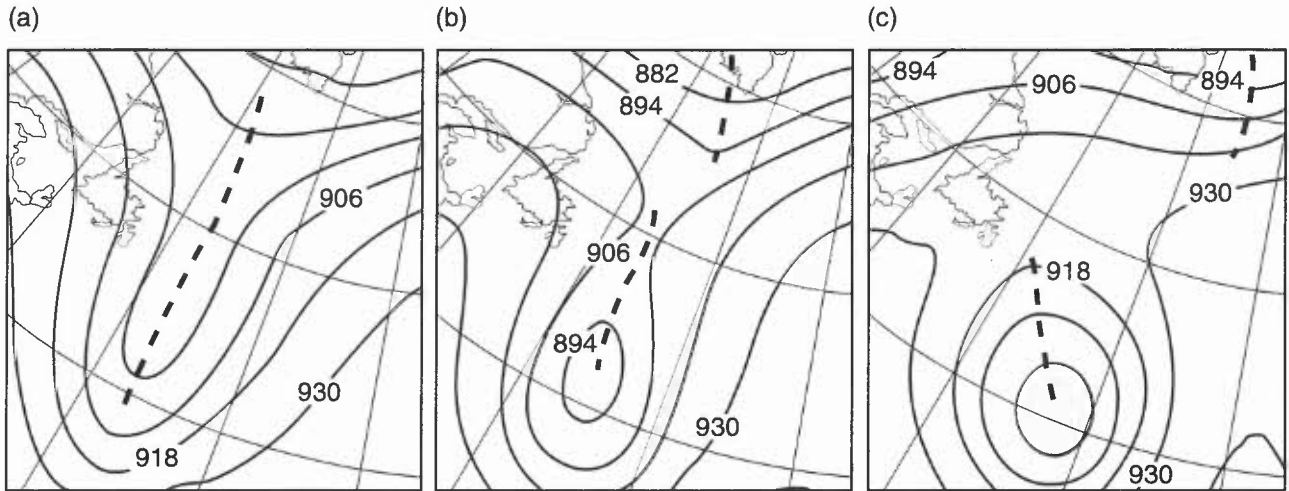


Figure 8.11. Trough disruption shown in 300 hPa gph forecast sequence. (a) T + 0 (00 UTC on 13 April 1995), (b) T + 12 (12 UTC on 13 April 1995), and (c) T + 24 (00 UTC on 14 April 1995).

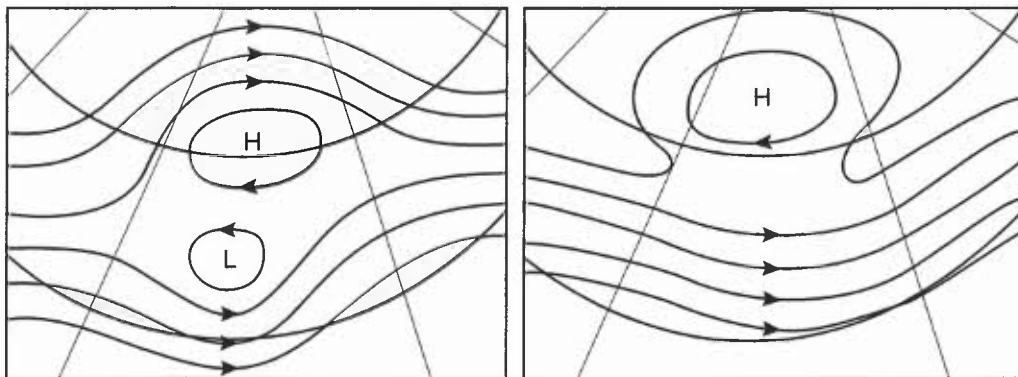


Figure 8.12. Schematic large-scale mid- or upper-tropospheric flow patterns in diffluent block (left) and omega block (right).

- (iv) Surface pressure rises across the neck of the disrupting trough, and the process is sometimes referred to as anticyclonic disruption.
- (v) Trough disruption is likely if the 300 hPa trough has an amplitude of 10° or more and if the jet has a strong equatorward component ($340\text{--}020^\circ$).
- (vi) The disruption process appears to be finely balanced, and the detail of such events is often not well predicted by NWP models.

8.4.5 Blocking

- (i) Blocking patterns give rise to prolonged periods when the normal mid-latitude zonal current is replaced over a large latitude range by meridional flow. A large, stationary high is the prominent feature of such situations.
- (ii) **Fig. 8.12** shows typical mid- to upper-tropospheric contour patterns associated with such situations. The usual latitudinal thickness gradient is reversed over a large area, with warm air cut off in high latitudes and pools of cold air in low latitudes.
- (iii) The normal westerly flow is either split into two equal streams as it flows around what is known as a diffluent block (**Fig. 8.12(a)**) or the westerly flow may be diverted to unusually low latitudes, forming what is known as an *omega block* (**Fig. 8.12(b)**).
- (iv) A block visible on charts is only part of a very large-scale, deep wave pattern.

8.5 Self development

8.5.1 Interaction of PVA with surface baroclinicity

A PVA area in a barotropic region progresses downstream without developing; development and amplification of surface and upper features will generally not take place unless a zone of surface baroclinicity is engaged, allowing constructive interaction between the two via positive feedback in the following way (**Fig. 8.13**):

- (i) Falling pressure ahead of an upper trough at a surface front brings warm and cold advection into play. Cold advection reinforces the upper trough, whilst warm advection helps build the downstream upper ridge.
- (ii) The intensification of the upper trough–ridge system increases the PVA, which further deepens the surface low, which increases the strength of the thermal advection, which further reinforces the upper wave and so on. The thermal advection configuration tends to strengthen the jet by shearing frontogenesis.
- (iv) The relative phase (trough/ridge positions) between the lower and upper troposphere is important. In a favourable ‘phase-locked’ conjunction a westward-tilting, developmental configuration is established, whereas advection of the upper feature ahead of the surface feature leads to mutual weakening (**Fig. 8.14**).
- (v) In the standard sequence of events, the occlusion process removes the PVA and low centre from the baroclinic zone, reducing thermal advection strength. In addition, the circulation becomes vertically uniform since there is a much reduced contribution from the thermal wind.
- (vi) The development of a closed circulation at upper levels above the surface feature reduces the PVA and makes the slope of the vorticity anomaly vertical. However, if baroclinicity can be maintained in the vicinity of the depression, e.g. by injection of fresh polar air, development can continue.
- (vii) Thermal advection by the lower tropospheric circulation is very important to the self-development process. For this reason, the tighter the pre-existing low-level thermal gradient, the greater the potential for cyclonic development. Preferred regions for cyclogenesis occur over oceanic areas of large sea-surface temperature gradient, such as the north-west Atlantic and north-west Pacific, or over cold continent/warm sea boundaries in winter.
- (viii) The temperature and humidity of the warm air mass is also important. High wet-bulb potential temperature air releases much latent heat on ascent, increasing upper-level divergence.
- (ix) The development process is not always initiated from aloft; the formation of a low-level perturbation can trigger the self-development process.

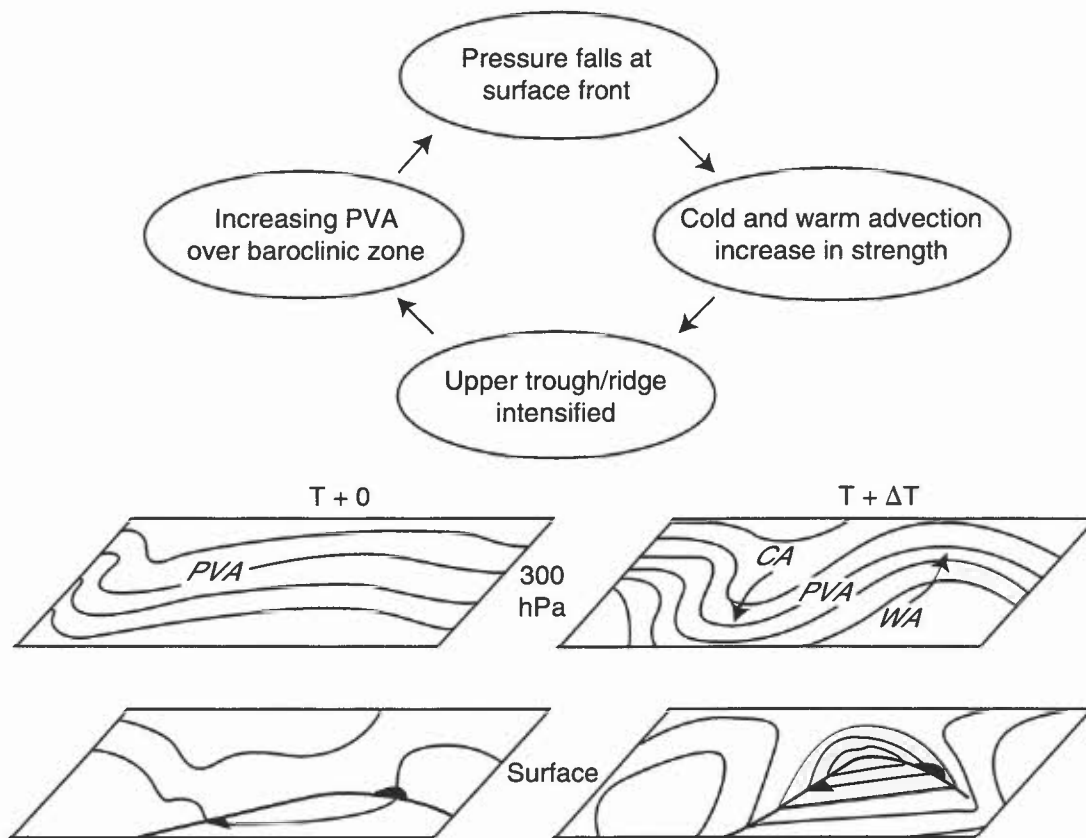


Figure 8.13. Self-development initiated by the engaging of a low-level baroclinic zone by an upper-level PVA region.

8.6 The quasi-geostrophic omega equation

8.6.1 Discussion

The diagnosis of vertical motion presented in sections 8.2 and 8.3 has the two-layer model as its basis, and is conceptual rather than mathematically rigorous. Quasi-geostrophic theory provides an objective framework for

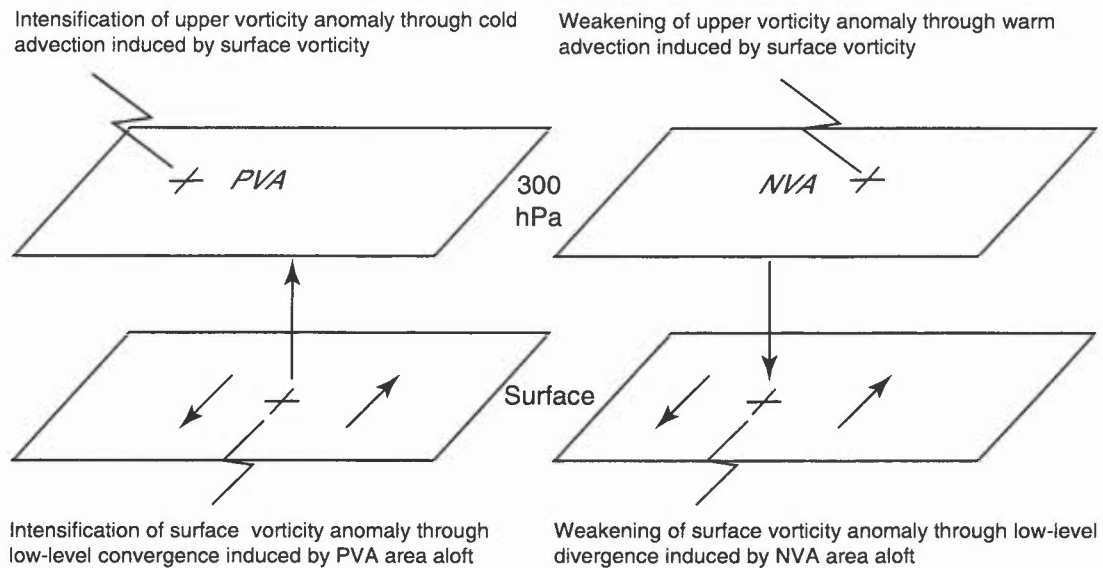


Figure 8.14. Self-developing (left) and self-destroying (right) configurations of surface and upper vorticity maxima.

calculating vertical velocity. It is based on simplified dynamics using the geostrophic advecting winds and other consistent approximations valid for synoptic-scale motion. One of its results, the omega equation, diagnoses the necessary vertical motion to adjust the vorticity and temperature fields into balance with each other in the face of thermal and vorticity advections. In its most well known form it can be given by

$$\frac{\partial^2 \omega}{\partial x^2} + \frac{\partial^2 \omega}{\partial y^2} + \frac{f^2}{\sigma} \frac{\partial^2 \omega}{\partial p^2} = \frac{f}{\sigma} \frac{\partial}{\partial p} \mathbf{V}_g \cdot \nabla_p (\zeta_g + f) + \frac{R}{\sigma p} \nabla_p^2 (\mathbf{V}_g \cdot \nabla_p T)$$

where σ is a stability parameter equal to $-1/(\rho\theta) \partial\theta/\partial p$ and ω is dp/dt , the vertical velocity in pressure co-ordinates. The form of the RHS determines the forcing, whilst that of the LHS determines the nature of the response.

Simply stated, upward (downward) motion is forced where there is PVA (NVA) in the upper troposphere and in the centres of warm (cold) advection regions, or where a region of cold (warm) advection borders on a region of little thermal advection.

However, applied subjectively it can give the wrong signal, and the following points are worth noting.

8.6.1.1 Interpretation: LHS

- (i) The LHS of the equation is a three-dimensional Laplacian of vertical velocity rather than vertical velocity itself. One way to visualize this is as the curvature in three dimensions of the vertical-velocity distribution.
- (ii) This Laplacian is negatively correlated with vertical velocity on the average, most reliably so near the level of non-divergence and in regions of strong ascent and descent.
- (iii) There is a scale dependence in the conversion of forcing to vertical velocity. Forcing from a small-scale feature such as a front translates to much less vertical velocity than forcing of the same strength from a feature such as a depression.
- (iv) The form of the equation shows ω to be dependent not just on local forcing but also on sources of forcing at a distance. The effect of forcing at lower levels is inhibited by the requirement that the vertical velocity should be small at the ground. Therefore, upper-tropospheric forcing is more influential than lower- to mid-tropospheric forcing of the same strength.
- (v) The only way to estimate vertical velocity with any certainty using the omega equation is by solving it with a computer. In doing so portions of the vertical velocity at any one level may be attributed separately to forcing from different levels.

8.6.1.2 Interpretation: RHS

- (i) Vertical velocity depends on the vertical variation of absolute vorticity advection and the Laplacian, or horizontal curvature, of the thermal advection field.

- (ii) Since vorticity advection generally increases in strength up to jet level, in mid-troposphere the vorticity advection term is strongest directly below the strongest upper-tropospheric vorticity advection.
- (iii) The Laplacian of the thermal advection field tends to be greatest in the centres of thermal advection regions, often with values of opposite sign at the edges of thermal advection anomalies.
- (iv) In addition, vertical motion is greater (less) in statically stable (unstable) air. The effects of latent heating can be absorbed into the stability parameter (assumed in the form given above) or treated more explicitly by a term in the Laplacian of heating.
- (v) In many situations there is a fair degree of cancellation between the terms, this cancellation increasing with the strength of the background flow — a strong PVA region embedded in a rapid westerly current, for instance, will probably be significantly offset by cold advection.
- (vii) The negative correlation between the Laplacian of vertical velocity and vertical velocity itself is often poor locally, but becomes better when integrated over a large volume. Therefore, subjectively it is best to apply a vertically integrated form, so that instead of temperature advection, thickness advection through a large depth of the atmosphere is used, and upper-level vorticity advection rather than its vertical variation is applied. The method then ends up being similar to the rules derived in 8.3.

8.6.2 Q-vector form

Hoskins et al. (1978) presented a version of the omega equation with only one forcing term. This has advantages over the form given earlier, entailing no cancellation and depending on no vertical derivatives.

$$\frac{\partial^2 \omega}{\partial x^2} + \frac{\partial^2 \omega}{\partial y^2} + \frac{f^2}{\sigma} \frac{\partial^2 \omega}{\partial p^2} = -2\nabla \cdot \mathbf{Q}$$

- (i) The vector \mathbf{Q} depends on the time rate of change of the potential temperature gradient due to horizontal variation of the geostrophic wind. This form of the omega equation above shows that forcing can be related to the divergence of the \mathbf{Q} field (not included in this rendering is the effect of the advection of planetary vorticity).
- (ii) Convergence (divergence) of \mathbf{Q} gives a forcing which would normally be associated with ascent (descent), though the points made under 8.6.1.1 still apply.
- (iii) \mathbf{Q} may be subjectively determined by noting the vector change in geostrophic wind along an isotherm in the direction of the thermal wind, turning this difference clockwise (in the NH) through 90° and multiplying it by the magnitude of the thermal wind (**Fig. 8.15**).
- (iv) \mathbf{Q} directed from cold (warm) to warm (cold) implies that frontogenesis (frontolysis) is occurring.

Fig. 8.16 shows a map of computer-generated \mathbf{Q} -vectors.

8.7 Sutcliffe theory

8.7.1 Discussion

Sutcliffe (1947) formulated a theory for predicting the tendency in surface vorticity based on the concept of a level of non-divergence at 500 hPa. His development equation can be manipulated to give

$$\frac{\partial}{\partial t} \zeta_{1000} \approx - (V_{1000} + \alpha V') \frac{\partial}{\partial s} \zeta_{1000} - \alpha V' \frac{\partial}{\partial s} (f + \zeta_{500})$$

where subscripts refer to the pressure levels and V' is the 1000–500 hPa thermal wind. α has an average value of 0.5, but increases towards 1 for very large or statically unstable systems and decreases towards 0 for very small systems or in situations of high static stability.

8.7.2 Interpretation

- (i) The local rate of change of vorticity at 1000 hPa is shown to be dependent on:
 - a steering term which is typically the wind at about half way between the 1000 and 500 hPa levels, say at 700 hPa;
 - a development term which is some proportion of the advection by the 1000–500 hPa thermal wind of the absolute vorticity at 500 hPa. This term on its own can be used to indicate the vertical velocity at 500 hPa (**Fig. 8.17**).

- (ii) As with the Q-vector omega equation, there is only one development term, allowing a clear signal in situations of cancellation between vorticity and thermal advection. The form given here is more accurate and involves much less cancellation than Sutcliffe's original form, which has as its development term the advection of thermal vorticity by the thermal wind.
- (iii) However, approximations made in the basic approach mean that whatever form is used, vertical velocity directly caused by deformation frontogenesis processes are not represented in Sutcliffe theory.

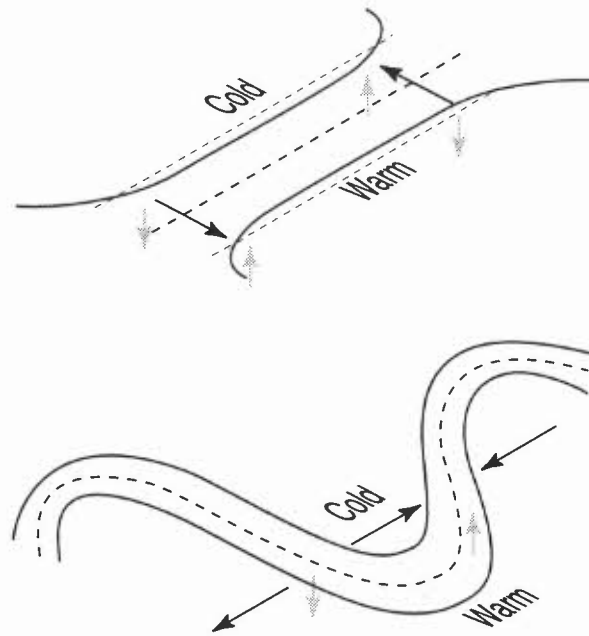


Figure 8.15. Q-vectors (dark arrows) associated with jet entrance and entrance patterns (top) and a ridge–trough–ridge pattern (bottom). Solid lines show geopotential, dashed lines temperature and light arrows implied vertical motion.

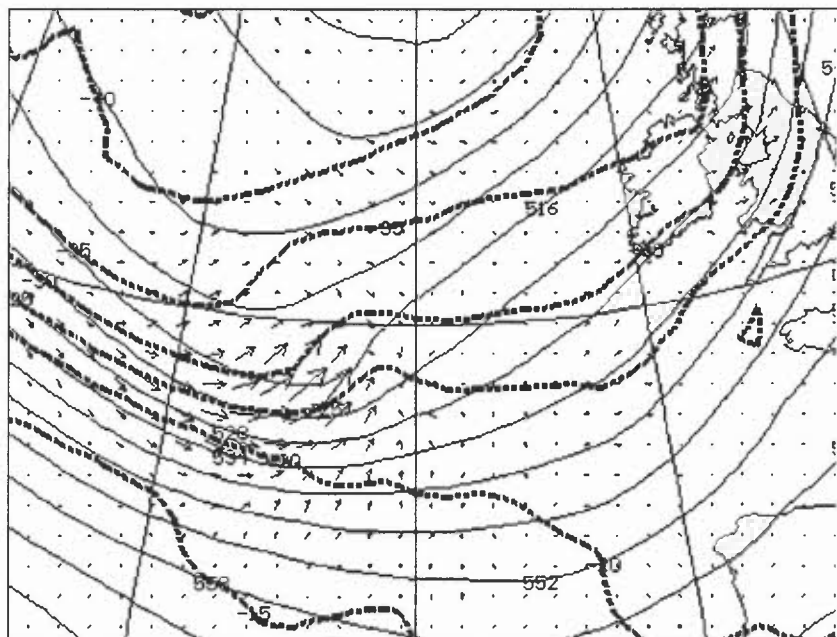


Figure 8.16. Forecast for 0000 UTC on 17 January 1995. Light solid contours show 500 hPa gph, dark dashed contours 500 hPa temperature, and Q-vectors.

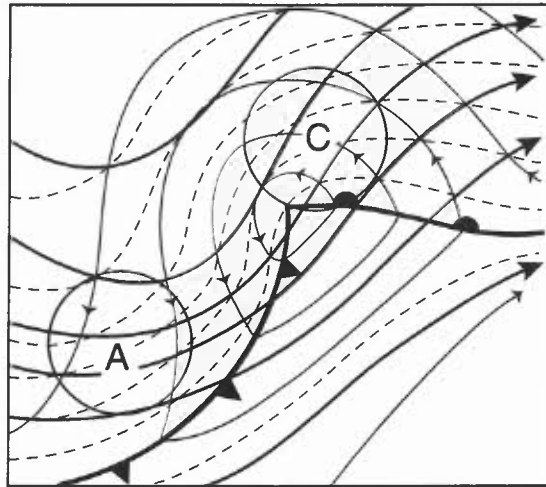


Figure 8.17. Schematic 500 hPa contours (dark solid lines), 1000 hPa contours (thin lines) and 1000–500 hPa thickness (dashed) illustrating a developing warm-sector depression. Sutcliffe development areas derived from advection of absolute vorticity by 1000–500 hPa thermal wind are marked.

8.8 Potential vorticity (PV)

8.8.1 Potential vorticity; conservation, invertibility

Potential vorticity can be expressed as

$$P = -g(\zeta_0 + f) \frac{\partial \theta}{\partial p}$$

where ζ_0 is the vorticity of the wind on an isentropic surface and $-\partial\theta/\partial p$ is a measure of static stability, being large in conditions of high stability. PV is conserved for frictionless, dry adiabatic processes, making it a good tracer for following features. It is also invertible, in the sense that a knowledge of PV distribution and boundary conditions allows other dynamic variables (e.g. temperature, geopotential wind) to be retrieved if some further balance conditions, such as geostrophic balance, is assumed.

8.8.1.1 Orographic and latitude effects

Fig. 8.18 shows how the effects of orography on stability and meridional motion on f can cause changes in the relative vorticity of the flow.

8.8.1.2 Units and representation

- (i) PV is usually measured in PV units, where 1 PV unit corresponds to $(\zeta + f) = 10^{-4} \text{ s}^{-1}$ and $\partial\theta/\partial p = 1 \text{ K per } 10 \text{ hPa}$.
- (ii) PV distribution is commonly either displayed as PV on an isentropic surface (e.g. $\theta = 315 \text{ K}$), as θ on a PV = 2 surface (i.e. the dynamic tropopause) or as the height of the PV = 2 surface. Low (high) θ or height correspond to high (low) PV on an isentropic surface.
- (iii) Unlike the other two measures, the height of the PV = 2 surface is not conserved following adiabatic, frictionless motion.

8.8.2 The PV view of development

- (i) PV features can be viewed as centres of forcing which induce a response in the geopotential height field remote from their locations, in a fashion which is broadly similar to the view of the omega equation presented in section 8.6.
- (ii) The strength of this remote effect is greatest with strong anomalies and in statically unstable air, and decreases with increasing distance.
- (iii) Because of the high static stability of the stratosphere, it has inherently high PV (>2 units), and anomalies close to the tropopause level are important for forcing development. An upper-level cyclonic PV anomaly draws lower-level isentropic surfaces upwards and apart, reducing static stability and inducing a cyclonic circulation below it (**Fig. 8.19**).

- (iv) Lower-tropospheric temperature anomalies can be thought of as PV anomalies concentrated in a thin layer at the surface, a warm (cold) region having the same effect as a positive (negative) PV anomaly. Dynamical development is controlled by the advection of internal PV anomalies and surface-temperature anomalies. However, since cold (warm) surface air is often associated with high (low) PV aloft, it is not unusual to have conflicting influences from above and below.
- (v) Cyclonic development occurs when a cyclonic upper PV anomaly engages a low-level baroclinic zone, initiating constructive interaction between the thermally induced surface circulation and the pre-existing upper trough in a way analogous to the self development described in 8.5 (Fig. 8.20).
- (vi) Vertical velocity can be thought of as arising from induced bulging of isentropic surfaces due to upper-level PV advection plus flow of air relative to the isentropic surfaces, i.e. thermal advection. Cyclonic (anticyclonic) PV advection at upper levels and warm (cold) advection lead to ascent (descent), but as with the traditional form of the omega equation, there can be cancellation.
- (vii) Latent heat release redistributes PV by warming mid-levels and changing stability, concentrating cyclonic PV at low levels and anticyclonic PV aloft.
- (viii) In some instances, stratospheric intrusions of dry, high PV air penetrate into the lower troposphere, causing marked cyclonic development at the surface.
- (ix) Ultimately, the ageostrophic motion, vorticity, omega equation and PV views, though apparently different, are nearly equivalent approaches to understanding development.

A cyclogenesis situation (Fig. 8.21) and a trough disruption situation (Fig. 8.22) are presented from the PV viewpoint.

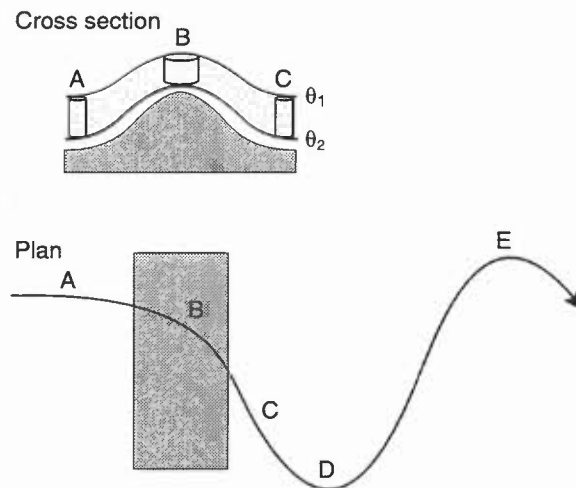


Figure 8.18. Orographic and meridional effects on flow deduced from principle of conservation of potential vorticity.
 A-B: $\partial\theta/\partial p$ increases in magnitude therefore ζ decreases.
 B-C: $\partial\theta/\partial p$ regains initial value therefore ζ increases.
 C-D: f increases therefore ζ increases.
 D-E: f increases therefore ζ decreases.

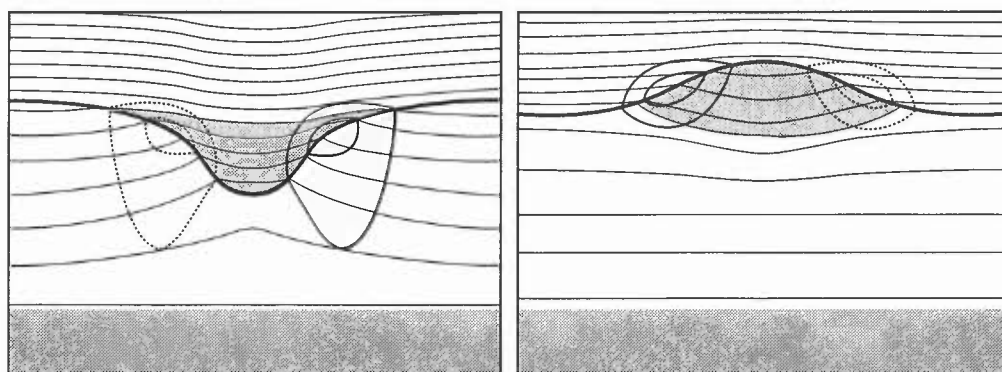


Figure 8.19. Cross-section of isentropes (thin lines, increasing in value upwards) and tropopause (thick line) associated with idealized upper-level PV anomalies, cyclonic (left) and anticyclonic (right). Also shown are anomaly positions (shaded) and isotachs (solid into page, dashed out of page).

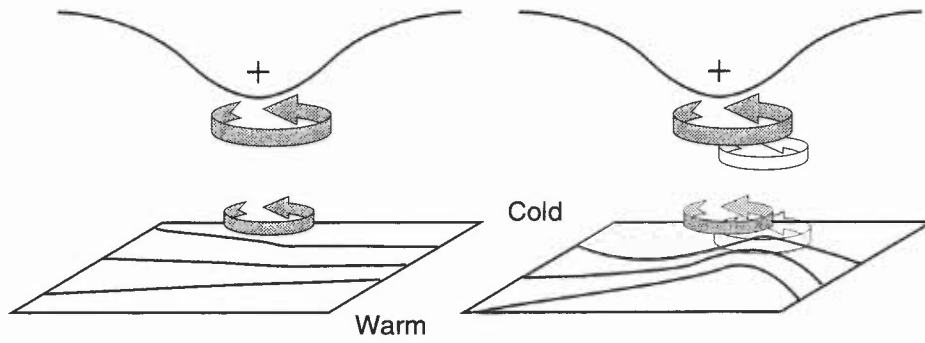


Figure 8.20. Schematic picture of cyclogenesis associated with the arrival of an upper PV anomaly over a low-level baroclinic zone. Dark line tropopause, thin lines surface isotherms. The low-level circulation induced by the cyclonic PV anomaly aloft advects warm air polewards. The resulting low-level warm anomaly induces a cyclonic flow at higher levels which advects high PV air equatorwards into the upper anomaly.

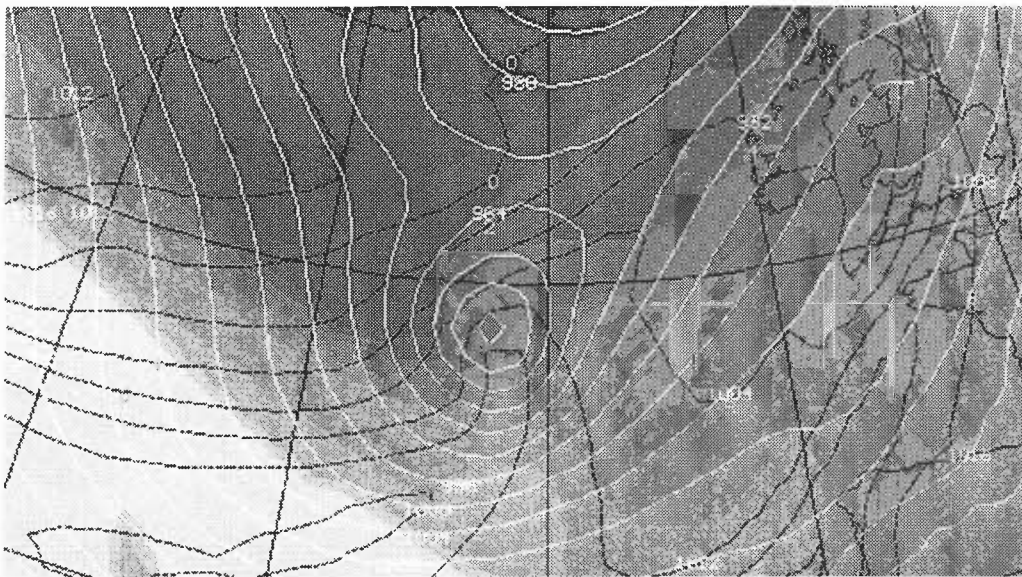


Figure 8.21. Forecast for 0000 UTC on 17 January 1995. Potential temperature on a $PV = 2$ surface shown by shade of background (dark cold, light warm, shades every 5°C); PMSL (light solid); 850 hPa wet-bulb potential temperature (dark dashed, every 2°C). Warm surface anomaly and upper positive PV anomaly combining to give strong forcing for cyclogenesis.

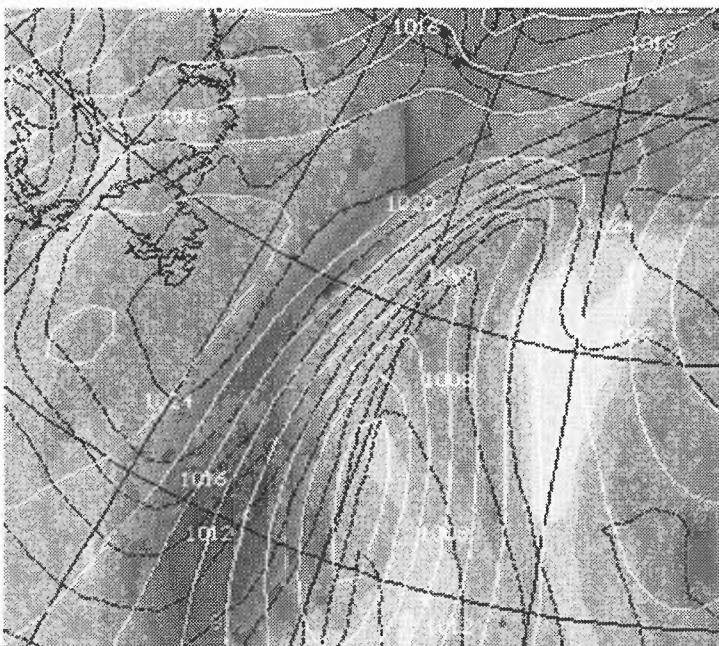


Figure 8.22. Forecast for 1200 UTC on 13 April 1995. Potential temperature on a $PV = 2$ surface, PMSL and 850 hPa wet-bulb potential temperature as in Fig. 8.21. The trough disruption case shown in Fig. 8.11. The surface depression lies close to a plume of warm air at low levels. The plunge of high PV aloft partly offset by advection of cold low-level air. Surface high south of Newfoundland forced by cold low-level air and low PV aloft.

BIBLIOGRAPHY

CHAPTER 8 — USE OF DYNAMICAL CONCEPTS IN ASSESSING DEVELOPMENT

- Bishop, C. and Thorpe, A.J. 1995: Potential vorticity and the electrostatics analogy. *QJR Meteorol Soc*, **120**, 713–731.
- Carlson, T.N., 1994: Mid-latitude weather systems. Routledge.
- Carroll, E.B., 1995: Practical subjective application of the omega equation and Sutcliffe development theory. *Meteorol Appl*, **2**, 71–81.
- Carroll, E.B., 1995: Diagnosis of a rapidly deepening depression: 16/17 January 1995. *Meteorol Appl*, **2**, 231–237.
- Clough, S.A., Davitt, C.S.A. and Thorpe, A.J., 1997: Attribution concepts applied to the omega equation (JCMM Internal Report 47). *QJR Meteorol Soc*, to be published.
- Durrant, D.R. and Snellman, L.W., 1987: The diagnosis of synoptic-scale vertical motion in an operational environment. *Weather and Forecasting*, **2**, 17–31.
- Hoskins, B.J., Draghici, I. and Davies, H.C., 1978: A new look at the ω -equation. *QJR Meteorol Soc*, **104**, 31–38.
- Hoskins, B.J., McIntyre, M.E. and Robertson, A.W., 1985: On the use and significance of isentropic potential vorticity maps. *QJR Meteorol Soc*, **111**, 877–946.
- Hoskins, B.J. and Pedder, M.A., 1980: The diagnosis of middle latitude synoptic development. *QJR Meteorol Soc*, **106**, 707–719.
- Sanders, F. and Hoskins, B.J., 1990: An easy method for the estimation of Q-vectors from weather maps. *Weather and Forecasting*, **5**, 346–353.
- Sutcliffe, R.C., 1947: A contribution to the problem of development. *QJR Meteorol Soc*, **73**, 370–383.
- Young, M.V., Browning, K.A. and Monk, G.A., 1987: Interpretation of satellite imagery of a rapidly deepening cyclone. *QJR Meteorol Soc*, **113**, 1089–1115.